JOURNAL OF Materials CHEMISTRY

Solid state chemistry of Fe–Ga mixed oxides

Jose Manuel Gallardo Amores,[a] Vicente Sanchez Escribano,[b] Guido Busca,[c] Enrique Fernandez Lopez[b] and Mohamed Saidi[a,d,e]

[a]*Dpto. Química Inorgánica. Lab. Complutense de Altas Presiones, U. Complutense, Ciudad Universitaria, E-28040 Madrid, Spain. E-mail: amores@eucmos.sim.ucm.es*
[b]*Dpto. Química Inorgánica, Universidad, Pl. de la Merced, E-37008 Salamanca, Spain.*
[c]*Dipartimento di Ingegneria Chimica e di Processo Bonino, Università, P. le J. F. Kennedy, I-16129 Genova, Italy.*
[d]*Dpt. de Génie Chimique, Faculté des Sciences et Techniques, Université Abdelmalek Essaadi, BP.416 Tangier, Maroc.*
[e]*Dpt. de Chimie, Faculté des Sciences, Université Abdelmalek Essaadi, BP.2121 Tétouan, Maroc.*

Received 19th April 2001, Accepted 24th July 2001
First published as an Advance Article on the web 18th September 2001

Several Fe–Ga mixed oxide samples denoted as $Fe_{1-x}Ga_x$ ($x=0$, 0.10, 0.25, 0.50, 0.75, 0.90) have been synthesised by a conventional coprecipitation method at controlled pH, dried at 363 K for 24 hours and calcined at 673 K and 1073 K for 3 hours. All samples were characterised by X-ray diffraction, chemical analyses, thermogravimetry and differential thermal analysis (TG-DTA) and FT-IR and UV-VIS spectroscopies. It was found all materials formed a solid solution, α-$(Fe,Ga)_2O_3$, in the entire Fe/Ga compositional range until 673 K. Samples calcined at 1073 K gave rise to biphasic systems for $x>0.5$ due to the different structure of β-Ga_2O_3 compared to α-Fe_2O_3. Surface acidity of samples was studied by pivalonitrile molecule adsorption on a pressed pellet of each material, and weak Lewis acidity was found in all cases, it not being possible to distinguish between both types of cation site on the surface, and Brönsted acidity that increased with increasing Ga content. Methanol molecules were also adsorbed, showing an increase of reactivity for those samples with very low Ga content.

Introduction

Gallium oxides present structures very similar to those of the α- and γ-series of their Al counterparts with almost equal stability ranges. However, β-Ga_2O_3 is, in this case, the most stable crystalline phase upon calcination at 873 K from α-Ga_2O_3.[1] The additional stability is attributed to preferential occupation of distorted tetrahedral and octahedral sites by Ga^{3+} ion in a distorted ccp structure of oxygen ions. This tendency is also observed for Fe^{3+} ions in the Fe_3O_4 structure.[2] As an immediate consequence the β-Ga_2O_3 structure is 10% less dense than the corundum structure, α-Ga_2O_3, which gives rise to solid solutions with many oxides of suitable cations.

As for its applications, Ga-based mixed oxides have been reported to be very active and selective catalysts in light alkane dehydrogenation.[3–5] These catalytic properties have attracted much attention and so Al–Ga mixed oxides have been used as catalysts with good performances in NO_x abatement by light hydrocarbons.[6] Also, Ga has been inserted in numerous zeolite frameworks in order to generate Brönsted acid sites.[7,8] It improves significantly the selectivity of these aluminosilicates in the catalytic conversion of olefins and paraffins to aromatics[9,10] and the Cyclar process where C_3–C_5 alkanes are transformed into aromatics and hydrogen. In previous works, we have studied Mn–Fe[11] and Al–Mn mixed oxides[12] as dehydrogenation catalysts and the resulting solid solutions with low Fe and Al contents exhibit notable improvements in catalytic activity and selectivity.

Nevertheless, few investigations have been performed to better know the solid state chemistry and surface of Fe–Ga mixed oxide system.[13] In earlier studies we have prepared mixed oxide systems of trivalent cations, such as Fe–Cr[14] and Al–Fe,[15,16] finding different grades of reciprocal solubility to depend mainly on cationic radius, and more recently Fe–Ga mixed precipitate powders[17] in order to improve the synthesis method and to produce thus better catalytic precursors.

In this work, we report our results on the structural characterization of several samples of the Fe–Ga mixed oxide systems with different Fe : Ga compositions synthesized by coprecipitation. Additionally, we have analyzed the surface by probe molecule adsorption in order to determine the acid site distribution and thus hypothesise potential catalytic applications.

Experimental

Samples have been prepared by coprecipitation, by mixing two aqueous solutions containing required amounts of the precursor salts $Fe(NO_3)_2{\cdot}9H_2O$ and $Ga(NO_3)_3{\cdot}9H_2O$ and adding $NH_4{\cdot}HCO_3$ up to pH = 7.5; then stirring continuously for 24 hours at 343 K, filtering and drying the gel at 393 K for 24 hours. A full characterization of the Fe–Ga hydroxides has been reported elsewhere.[18] Nitrates and residual organic compounds were decomposed, in air, in a furnace at 673 K for 3 hours and finally separate portions of each sample were calcined in air at 1073 and 1273 K for 3 hours. Samples will be denoted hereinafter as $Fe_{1-x}Ga_x$ (with $x=0$, 0.10, 0.25, 0.50, 0.75, 0.90). The chemical analyses were performed with a Plasma II Perkin-Elmer emission spectrometer after dissolution of the precipitates in an HF–HNO_3 mixture. Experimental data are in very close agreement with the sample nominal composition (Fe/Ga experimental atomic ratio: 1, 8.92, 3.06, 0.97, 0.31, 0.13, 0; Fe/Ga nominal atomic ratio: 1, 9, 3, 1, 1/3, 1/9, 0).

The XRD spectra were recorded on a Siemens D-500 diffractometer (Cu Kα radiation, Ni filter; 35 kV, 35 mA). Cell

 DOI: 10.1039/b103523c

parameters were calculated with dedicated least squares software.

The FT-IR spectra were recorded using a Nicolet Magna 750 Fourier Transform instrument. For the region 4000–350 cm^{-1} a KBr beam splitter was used with a DTGS detector. For the FIR region (600–50 cm^{-1}) a "solid substrate" beam splitter and a DTGS polyethylene detector were employed. KBr pressed disks (IR region) or a polyethylene solid support (FIR region) were used. The FT-IR spectra arising from pivalonitrile adsorption over pressed disks of each sample pretreated at 623 K were recorded after outgassing upon heating at different temperatures.

The UV-VIS spectra were recorded with a Jasco V-570 spectrophotometer in the region 200–2500 nm using pressed disks of the samples and a polymer as a reference.

Results and discussions

Characterization of powders upon calcination at 673 K

XRD. As reported in a previous study,[18] the Fe–Ga mixed hydroxides decompose at 673 K giving rise to monophasic materials in the entire compositional range, denoted as α-$(Fe,Ga)_2O_3$, with significant variations of crystallinity. This is due to the isomorphous structural character of both pure oxides (α-Fe_2O_3, ICDD no. 33-664 and α-Ga_2O_3, ICDD no. 6-503) and the similar cationic radii.[18] We show in Table 1, as a resume of this previous study, the cell parameters, volume and % Fe in α-Ga_2O_3 of Fe–Ga samples calcined at 673 K. The behavior of the Fe–Ga mixed oxides is confirmed by the unit cell parameters and volume calculated for all samples (Table 1). The volume tends to increase, in parallel with the *c* parameter, with increasing iron content according to the higher Fe^{3+} radius and suggesting a continuous substitution between both cations in the corundum type structure. Meanwhile, the *a* parameter varies irregularly, giving rise to small variations of volume. The % Fe in the α-Ga_2O_3 structure has been calculated by application of Vegard's law. This procedure allows, for a wide range of mixed oxide systems, reciprocal solubilities to be calculated successfully, but some deviations are also known.[19] Thus, at low Ga contents, theoretical values from the virtual composition are in agreement with the Fe solubility in α-Ga_2O_3, while some deviations are found for values calculated from the *a* unit cell parameter for higher Fe contents.

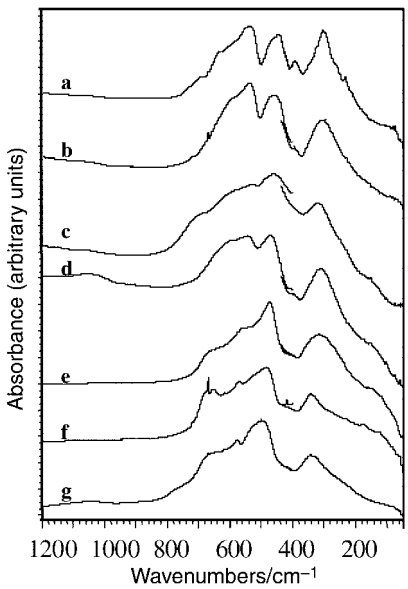

Fig. 1 FT-IR spectra of powders calcined at 673 K. a) Fe, b) $Fe_{1.8}Ga_{0.2}$, c) $Fe_{1.5}Ga_{0.5}$, d) $Fe_{1.0}Ga_{1.0}$, e) $Fe_{0.5}Ga_{1.5}$, f) $Fe_{0.2}Ga_{1.8}$ and g) Ga.

Skeletal FT-IR spectroscopy. The FT-IR spectrum of the Fe sample shows well-defined absorption bands near 233, 303, 392, 444 and 535 cm^{-1} and two shoulders near 667 and 691 cm^{-1} (Fig. 1), assigned to α-Fe_2O_3, in good agreement with the spectra reported elsewhere.[15,20] Upon adding Ga, all features shift to higher wavenumbers and change significantly in shape becoming more broad, and the weaker signals become indistinguishable from the $Fe_{1.5}Ga_{0.5}$ sample (Fig. 1c), according to the crystallinity loss reported in XRD. Similar effects have already been reported in Fe–Al systems[15] and they are associated with progressive Fe substitution by Ga in the structure. For the 1 : 1 Fe : Ga composition, the spectrum is still similar to that of the Fe sample with three main features at 544, 470 and 322 cm^{-1}, but higher Ga content causes a marked transformation in the spectrum with the band at 470 cm^{-1} increasing in intensity (Fig. 1e) and the bands attributed to the α-Ga_2O_3 phase becoming distinguishable. All of them are identified from the $Fe_{0.2}Ga_{1.8}$ sample, whose spectrum is

Table 1 Cell parameters, volume and % Fe in the α-Ga_2O_3 structure calculated by Vegard's law for Fe_xGa_{1-x} samples calcined at 673, 1073 and 1273 K

T/K	Phase/C.P./%S	Ga α-Ga_2O_3	$Fe_{0.2}Ga_{1.8}$ α-$(Fe,Ga)_2O_3$	$Fe_{0.5}Ga_{1.5}$	$Fe_{1.0}Ga_{1.0}$	$Fe_{1.5}Ga_{0.5}$	$Fe_{1.8}Ga_{0.2}$	Fe α-Fe_2O_3
673	$a=b$/Å	4.984(0)	4.987(2)/7	4.998(4)/35	4.990(10)	4.993(1)	5.025(2)	5.024(1)
	c/Å	13.452(1)	13.475(6)/8	13.503(14)/18	13.659(21)/73	13.709(20)/91	13.731(10)/98	13.736(3)
	V/Å^3	289.4	290.3	292.2	294.5	295.9	300.7	300.3
	Phase/C.P./%S	β-Ga_2O_3		β-Ga_2O_3/α-Fe_2O_3		α-Fe_2O_3		
1073	a/Å	5.802(7)	5.803(4)	5.823(13)	5.802(9)			
	b/Å	3.039(4)	3.043(3)	3.048(5)	3.036(9)			
	c/Å	12.225(18)	12.251(25)	12.875(23)	12.199(18)			
	V/Å^3	209.5	210.2	210.5	209.1			
	$a=b$/Å			5.014(5)	5.029(8)	5.024(4)	5.022(3)	5.029(2)
	c/Å			13.525(22)/27	13.570(35)/44	13.688(14)/88	13.699(15)/92	13.721(13)
	V/Å^3			294.4	297.2	299.2	299.4	300.5
	Phase/C.P./%S		β-Ga_2O_3		$GaFeO_3$	α-Fe_2O_3		
1273	a/Å		5.823(6)	5.830(10)	8.718(9)	5.031(2)	5.018(7)	
	b/Å		3.043(4)	3.056(6)	9.390(13)	5.031(2)	5.018(7)	
	c/Å		12.239(11)	12.284(17)	5.069(5)	13.661(6)/78	13.765(22)	
	V/Å^3		210.6	212.1	414.9	299.4	300.2	

Note: %S = %Fe in α-Ga_2O_3; C.P. = cell parameter.

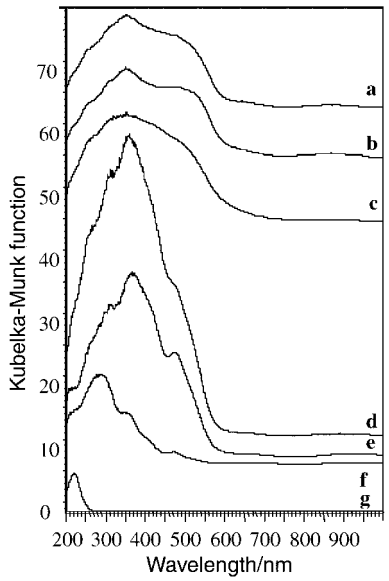

Fig. 2 Electronic spectra in the UV-VIS region of powders calcined at 673 K. a) Fe, b) $Fe_{1.8}Ga_{0.2}$, c) $Fe_{1.5}Ga_{0.5}$, d) $Fe_{1.0}Ga_{1.0}$, e) $Fe_{0.5}Ga_{1.5}$, f) $Fe_{0.2}Ga_{1.8}$ and g) Ga.

practically analogous to that of the Ga sample. The latter presents absorption bands near 343, 497, 576, 668 and 775 (shoulder) cm^{-1} in good agreement with the spectra previously reported by Burkholder *et al.*[21]

Electronic spectra. As reported in Fig. 2, the UV-VIS spectrum of the Fe sample displays a main absorption at 352 nm with additional shoulders near 252, 450 and 515 nm. Weaker features are found at higher wavelengths near 641 and 869 nm. According to previous studies,[22] the absorption bands at 252 and 515 nm can be related reasonably to $O^{2-}\rightarrow Fe^{3+}$ and $Fe^{3+}\rightarrow Fe^{3+}$ charge-transfer of octahedral Fe^{3+}, respectively. Meanwhile, the features at 641 and 869 nm can appear or not depending on the synthesis method,[14,23] and are related to Fe^{3+} in an octahedral environment on the surface. Otherwise, the bands at 352 and 450 nm have a more difficult interpretation since their positions vary significantly as a function of Fe^{3+} compound.

This spectrum is modified substantially by increasing the Ga content, resulting in a broad absorption maximum near 352 nm for the 1.5 : 0.5 Fe : Ga composition (Fig. 2c) which can not be related to the presence of Ga if the spectrum of the Fe-free sample is observed. Thus, these spectra can be explained as electronic transitions implying that the Fe^{3+} cations are in an environment which may be influenced by the presence of Ga^{3+} due to the difference between the radii of Fe^{3+} and Ga^{3+} cations (X and Y, respectively), in good agreement with previous works.[13] Further increasing the Ga content has a notable influence on the intensity of the spectral features described above (Fig. 2d); then from $Fe_{1.5}Ga_{0.5}$ the intensity decreases once more until practically no absorption bands are visible in the Ga sample. The band situated at 237 nm in this last spectrum is probably due to oxygen absorption as a consequence of the experimental conditions. The behavior of the Ga-rich samples can be clearly related to an effect of isolation of Fe^{3+} cations in the β-Ga_2O_3 structure, which tends to make all the features of the Fe^{3+} electronic spectrum disappear, as observed by us in the Al–Fe oxide system.[15,16]

Characterization of powders upon calcination at 1073 K

XRD. The behavior of the materials calcined at 1073 K is shown in Fig. 3. In general, calcination at 1073 K has resulted in notably increased crystallinity for all the samples without significant variations between them, as already observed at

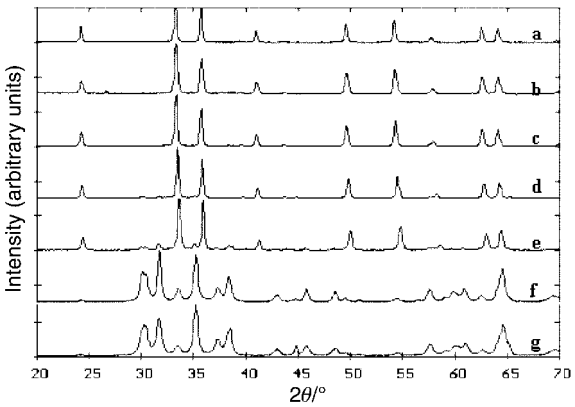

Fig. 3 XRD patterns of powders calcined at 1073 K. a) Fe, b) $Fe_{1.8}Ga_{0.2}$, c) $Fe_{1.5}Ga_{0.5}$, d) $Fe_{1.0}Ga_{1.0}$, e) $Fe_{0.5}Ga_{1.5}$, f) $Fe_{0.2}Ga_{1.8}$ and g) Ga.

673 K. Unique phases are found for the pure Fe and Ga samples, attributed to α-Fe_2O_3 (ICDD, no. 33-664) and to β-Ga_2O_3 (ICDD, no. 11-370), respectively. Meanwhile, the XRD patterns for the Fe–Ga mixed oxide samples from $Fe_{1.8}Ga_{0.2}$ to $Fe_{1.0}Ga_{1.0}$ (Fig. 3a–d) are consistent with an α-Fe_2O_3 phase with a high Ga^{3+} content, denoted as α-$(Fe,Ga)_2O_3$ above. Otherwise, the samples with higher Ga contents are biphasic, fully consistent with α-$(Fe,Ga)_2O_3$ and β-Ga_2O_3 phases. For $Fe_{0.5}Ga_{1.5}$ (Fig. 3e), the α-$(Fe,Ga)_2O_3$ phase is still present in a higher percentage than Ga, as seen qualitatively from intensity values, but further increasing the Ga content dramatically changes this ratio (Fig. 3f).

Unit cell parameters and volumes of the samples are reported in Table 1. They display a tendency to decrease with increasing Ga content until 0.5 : 1.5 Fe : Ga, indicating the formation of a solid solution in this composition range. The solubility of Ga in the Fe_2O_3 structure, calculated from the *c* parameter by Vegard's law, is for all samples very similar to the virtual composition (Table 1). Then, the appearance of a new non-isostructural phase, β-Ga_2O_3, prevents further exchange between the cations by diffusion and no variations are observed in the cell parameters for samples richer in Ga. Therefore, increasing the temperature significantly improves the solubility of Ga in α-Fe_2O_3.

In order to establish the stability range of the above solid solutions, the samples were calcined at 1273 K (Fig. 4). The XRD patterns resemble, in part, the picture described at 1073 K, *i.e.*, solid solutions denoted as α-$(Fe,Ga)_2O_3$ occur up to the $Fe_{1.5}Ga_{0.5}$ sample. Beyond this composition, the XRD pattern changes completely and a new phase appears for 1 : 1 Fe : Ga (Fig. 4d), fully consistent with the perovskite $GaFeO_3$

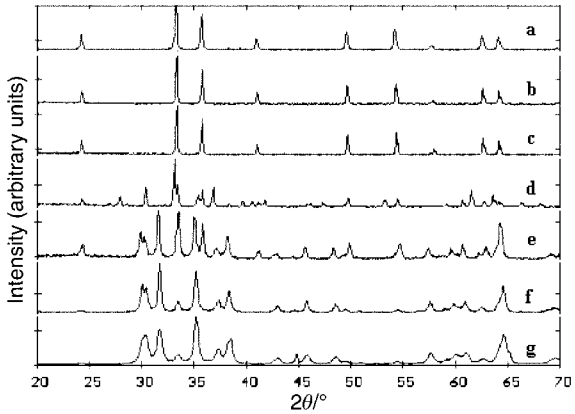

Fig. 4 XRD patterns of powders calcined at 1273 K. a) Fe, b) $Fe_{1.8}Ga_{0.2}$, c) $Fe_{1.5}Ga_{0.5}$, d) $Fe_{1.0}Ga_{1.0}$, e) $Fe_{0.5}Ga_{1.5}$, f) $Fe_{0.2}Ga_{1.8}$ and g) Ga.

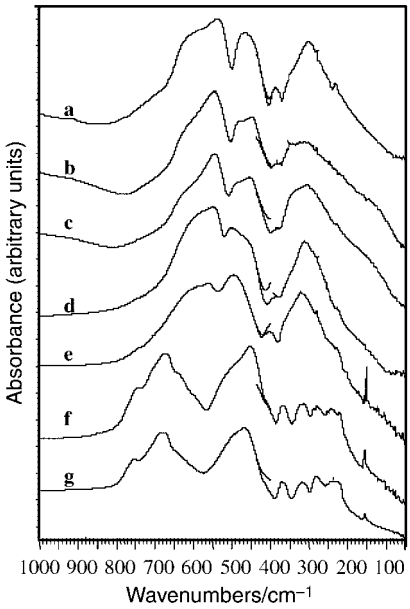

Fig. 5 FT-IR spectra of powders calcined at 1073 K. a) Fe, b) $Fe_{1.8}Ga_{0.2}$, c) $Fe_{1.5}Ga_{0.5}$, d) $Fe_{1.0}Ga_{1.0}$, e) $Fe_{0.5}Ga_{1.5}$, f) $Fe_{0.2}Ga_{1.8}$ and g) Ga.

phase (ICDD no. 26-673). This fact is due to the stoichiometric reaction between the two oxides:

$$Ga_2O_3 + Fe_2O_3 \rightarrow 2FeGaO_3 \quad (1)$$

$FeGaO_3$ is still present together with β-Ga_2O_3, as a minor constituent, for the $Fe_{0.5}Ga_{1.5}$ sample and suddenly disappears for lower Fe contents. Therefore, Fe^{3+} remains in the β-Ga_2O_3 structure giving rise to a solid solution for Fe contents lower than 10% at 1273 K.

Skeletal FT-IR spectroscopy. The FT-IR spectra of samples calcined at 1073 K are compared in Fig. 5. The spectrum of the Fe oxide sample is similar to that discussed at 673 K but with slightly increased intensity and so better resolved bands are found (Fig. 5a). The addition of Ga induces a progressive loss of intensity until the $Fe_{1.5}Ga_{0.5}$ sample, with a parallel shift of all vibrational modes towards higher wavenumbers. The FIR region loses resolution and no bands are distinguished. Additionally, a new band becomes defined at 497 cm^{-1} and it is assigned to β-Ga_2O_3 by comparison with other spectra. These modifications are due to changes in the shape and size of particles, as discussed in XRD where a progressive broadening of peaks is described. Further Ga addition (Fig. 5d and e) leads to transitional spectra in which typical features of the β-Ga_2O_3 phase are not defined yet. In particular, the FIR region presents a unique band at 311 cm^{-1}. For the composition 0.2 : 1.8 Fe : Ga the picture changes fully with all adsorption bands attributed to the β-Ga_2O_3 phase becoming visible, in agreement with the XRD patterns. This spectrum and that of the Ga sample are completely consistent with those reported elsewhere.[24,25]

Electronic spectra. The electronic spectra of samples calcined at 1073 K are shown in Fig. 6. For the Ga-free sample, all features agree with the assignments previously discussed at 673 K. Only the band at about 450 nm ($^6A_1 \rightarrow {}^4T_2({}^4D)$, tetrahedral Fe^{3+}) is not clearly identified; upon further calcinations it is found to be probably due to the α-Fe_2O_3 structure. However, the Ga containing samples decrease notably in intensity, though the trend of absolute intensity is similar to that of the samples calcined at 673 K. As a consequence, the absorption bands at 450 and 515 nm overlap for low Ga contents (Fig. 6b and c) and they transform into

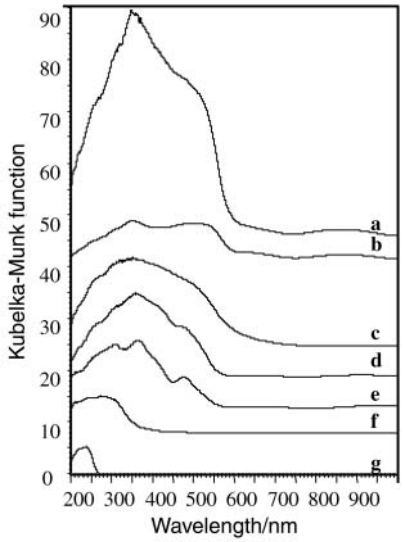

Fig. 6 Electronic spectra in the UV-VIS region of powders calcined at 1073 K. a) Fe, b) $Fe_{1.8}Ga_{0.2}$, c) $Fe_{1.5}Ga_{0.5}$, d) $Fe_{1.0}Ga_{1.0}$, e) $Fe_{0.5}Ga_{1.5}$, f) $Fe_{0.2}Ga_{1.8}$ and g) Ga.

only a well-defined band at about 450 nm when the amount of added Ga^{3+} increases. This behavior suggests that Ga^{3+} acts to isolate Fe^{3+} in the α-Fe_2O_3 structure and therefore Fe^{3+} intercationic transitions are prevented, as seen in analogous systems.[15,16]

Otherwise, the features of the β-Ga_2O_3 phase start to be identified from the 1 : 1 Fe : Ga composition in the XRD pattern and FT-IR spectra. On the other hand, Fe^{3+} exhibits a tendency to occupy tetrahedral sites in the mixed samples, as deduced from the intensity increase of the band at about 480 nm assigned to tetrahedral Fe^{3+}. This fact indicates that, in contrast to the iron sample, in the solid solution structure Fe^{3+} ions also occupy tetrahedral coordination sites, as reported for spinel-type structures.[13]

Surface characterization of samples calcined at 673 K

Study of the hydroxyl groups on the surface. Fig. 7 shows the spectra of the surface hydroxyl groups on all samples, in particular, those of Fe oxide and Ga oxide have been pretreated at 623 and 673 K. Upon outgassing at 623 K, six bands become

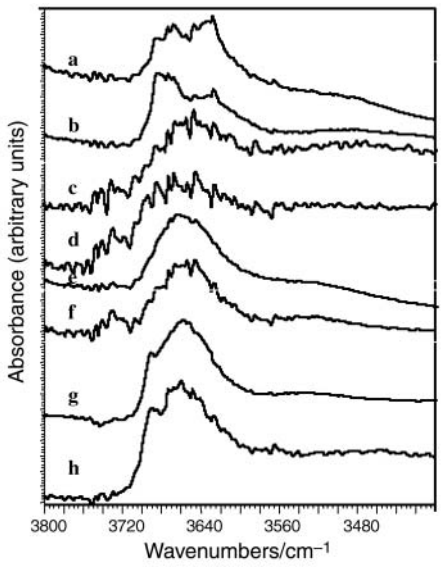

Fig. 7 FT-IR spectra of powders activated previously at 623 K. a) Fe (623 K), b) Fe (673 K), c) $Fe_{1.8}Ga_{0.2}$, d) $Fe_{1.5}Ga_{0.5}$, e) $Fe_{1.0}Ga_{1.0}$, f) $Fe_{0.5}Ga_{1.5}$, g) $Fe_{0.2}Ga_{1.8}$ and h) Ga (623 and 673 K).

evident in the spectrum for the pure Fe sample (Fig. 7a) at 3684 (shoulder), 3667, 3646, 3627, 3590 (shoulder) and 3480 (shoulder) cm^{-1}. The two bands at lower wavenumbers disappear upon further heating to 673 K, while the relative absorbances for the other bands are inverted. As reported previously,[16,26] the former, lower wavenumber bands are typical of α-Fe_2O_3, haematite, and are attributed to stable free OH groups (terminal OHs on octahedral cations and bridging OHs) and hydrogen-bonded, possibly clustered, hydroxyl groups, respectively. The addition of small amounts of Ga decreases significantly the transmittance in this region, and the spectrum appears very perturbed. However, it is still possible to distinguish three hydroxyl groups at about 3731, 3666 and 3647 cm^{-1}. Only that at higher wavenumbers is assignable to traces of γ-Fe_2O_3, maghemite, concentrated on the surface in agreement with the poorly crystalline materials found in XRD patterns. γ-Fe_2O_3 is a typical impurity in this kind of synthesis,[15] though it was not identified by XRD. For the 1:1 Fe:Ga sample, the spectrum once again becomes more resolved (Fig. 7e), with two bands at 3665 and 3646 (shoulder) cm^{-1} being identified as well as another weaker one at 3540 cm^{-1}, which are still analogous to those of α-Fe_2O_3 discussed above. Upon further Ga addition, the position and intensity of the bands due to hydroxyl groups start to be similar to those of the Ga sample. This surface is characterized by two kinds of well defined OHs at 3690 and 3660 (stronger) cm^{-1} shifted by *ca.* 20 cm^{-1} with respect to those of α-Fe_2O_3. Therefore, the surfaces of the samples change significantly when Ga is added, with OH groups on octahedral cations and bridging OH groups being present, the latter being present in greater proportion.

Study of the adsorption of pivalonitrile. In previous papers it has been shown that very weak bases such as nitriles (CN) can be used for the study of strong Lewis acid sites.[27,28] The CN group interacts with a cation or OH group on the catalyst surface, shifting the CN stretching band in agreement with the acid site strength. Meanwhile, interactions with the free OH groups produce a shift of the sharp ν_{OH} band to lower wavenumbers, as a measure of the Brönsted acidity.

Taking into account the above comments, the FT-IR spectra arising from pivalonitrile adsorption for all Fe–Ga oxide samples (previously activated at 673 K) before and after outgassing at r.t. are compared in Fig. 8A and B, respectively. Only a band at 2235 cm^{-1} is found in the FT-IR spectrum for pivalonitrile vapor (Fig. 8A), which shifts toward higher wavenumbers and loses intensity significantly after interacting with the samples with a Ga content <0.5 (Fig. 8A, a–b). For higher Ga contents, an additional band appears at about 2268 cm^{-1}, which shifts to higher wavenumbers with increasing Ga content, and becomes more intense than that at 2236 cm^{-1} for the Ga oxide sample where a splitting is observed (Fig. 8A, g). By comparison with the pivalonitrile vapor spectrum (Fig. 8A), the bands can be related to physisorbed pivalonitrile species (2244 cm^{-1}) and to an interaction with a unique Lewis acid site (2274 cm^{-1}), except for the Ga oxide sample where at least two types of Lewis acid sites are found at 2278 cm^{-1} and 2268 cm^{-1}. These data are in good agreement with the picture shown in the OH group study. After outgassing at r.t. (Fig. 8B), samples with a low Ga content (Fig. 8B, a–c) do not show the band at lower wavenumbers suggesting the elimination of physisorbed pivalonitrile. On the other hand, in the samples with high Ga content the band at 2274 cm^{-1} remains and increases progressively in intensity together with a small shoulder at 2239 cm^{-1} for the $Fe_{0.5}Ga_{1.5}$ and $Fe_{0.2}Ga_{1.8}$ samples. Meanwhile, an additional strong band appears at 2201 cm^{-1} in the $Fe_{1.0}Ga_{1.0}O_y$ sample. Further temperature increases produce the disappearance of all bands observed at 423 K. These data suggest that the strength of Lewis acidity increases with the Ga content, situating the band at 2274 cm^{-1} between those reported previously for V_2O_5 (2280 cm^{-1}) and for TiO_2 anatase (2265 cm^{-1}). Accordingly, Lewis acid sites are weak because all pivalonitrile molecules are evacuated in the 423–473 K temperature range.[29]

The mode of pivalonitrile adsorption is found to be vertical as observed in Fig. 9A, where no perturbations are observed in the CH stretching and deformation region between the peaks corresponding to pivalonitrile vapor and the other ones. Finally, FT-IR spectra in the OH stretching region are compared after pivalonitrile adsorption at r.t. for all samples in Fig. 9B. The ν_{OH} stretching band shifts to lower wavenumbers from 3650 cm^{-1} for the Fe oxide sample (Fig. 9B, h) to 3350 cm^{-1} for the samples with low Ga content (Fig. 9B, a). This fact indicates the occurrence of Brönsted acidity on the sample surface which tends to increase when the Ga content increases[29] up to the $Fe_{0.5}Ga_{1.5}$ sample. Moreover, for these samples at least two types of Brönsted acid sites can be identified at about 3500 and 3380 cm^{-1} (Fig. 9B, d–f), while for samples with high Fe content (Fig. 9B, b,c) the OH stretching region appears fully unresolved in good agreement with the crystallinity losses discussed in XRD analyses. For samples with high Ga content (Fig. 9B, g), Brönsted acidity disappears almost totally (Lewis acidity is predominant on the surface as explained above) and Ga_2O_3 hydroxyl groups on the surface

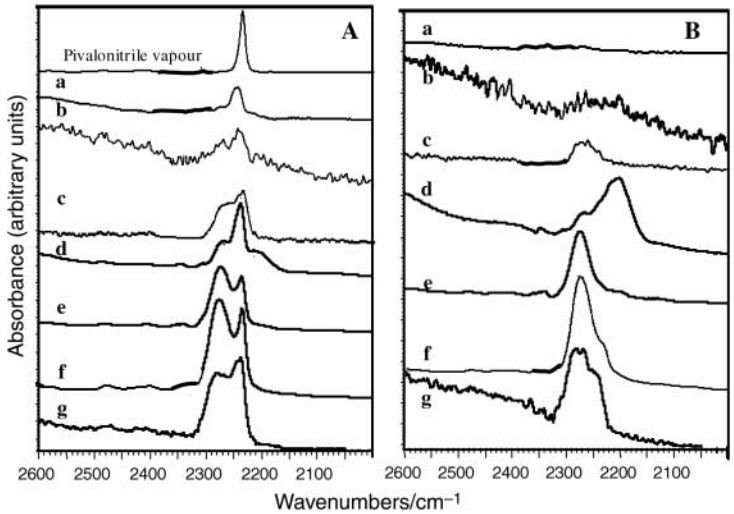

Fig. 8 FT-IR spectra arising from pivalonitrile adsorption for all powders at r.t. before (A) and after outgassing (B). a) Fe, b) $Fe_{1.8}Ga_{0.2}$, c) $Fe_{1.5}Ga_{0.5}$, d) $Fe_{1.0}Ga_{1.0}$, e) $Fe_{0.5}Ga_{1.5}$, f) $Fe_{0.2}Ga_{1.8}$ and g) Ga.

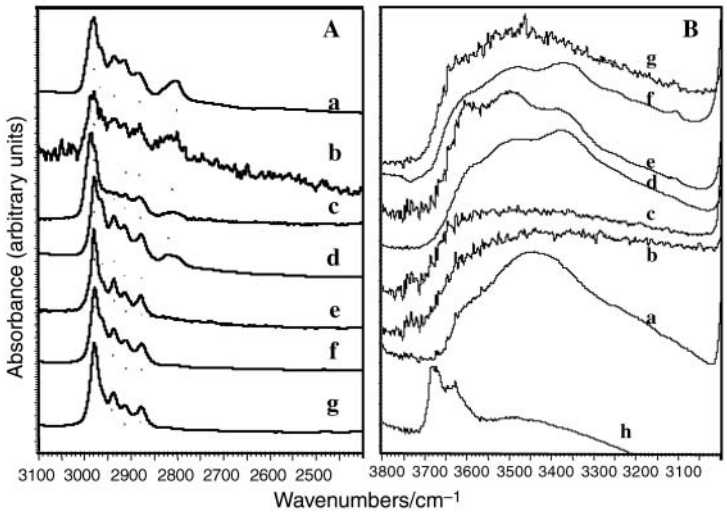

Fig. 9 FT-IR spectra arising from pivalonitrile adsorption for all powders in the CH (A) and OH (B) stretching regions at r.t. a) Fe, b) $Fe_{1.8}Ga_{0.2}$, c) $Fe_{1.5}Ga_{0.5}$, d) $Fe_{1.0}Ga_{1.0}$, e) $Fe_{0.5}Ga_{1.5}$, f) $Fe_{0.2}Ga_{1.8}$, g) Ga and h) Fe sample before the pivalonitrile adsorption.

are again observed in this region and are shifted upwards with respect to those for the Fe_2O_3 sample (see Fig. 7). This behavior was also observed in α-(Fe,Ga)OOH[18] and it is related to the ionic potential increase in the Ga^{3+} cation which tends to make the Ga–O bond distance and also the vibration frequency between Ga and O atoms decrease.

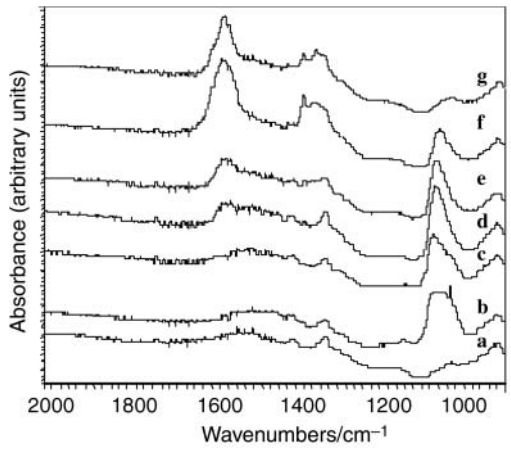

Fig. 10 FT-IR spectra arising from methanol adsorption on the $Fe_{1.8}Ga_{0.2}O_y$ sample in the 900–2000 cm^{-1} region at different temperatures. a) Activation at 623 K, b) r.t., c) ev. 373 K, d) ev. 423 K, e) ev. 473 K, f) ev. 523 K and g) ev. 573 K (ev. = outgassing).

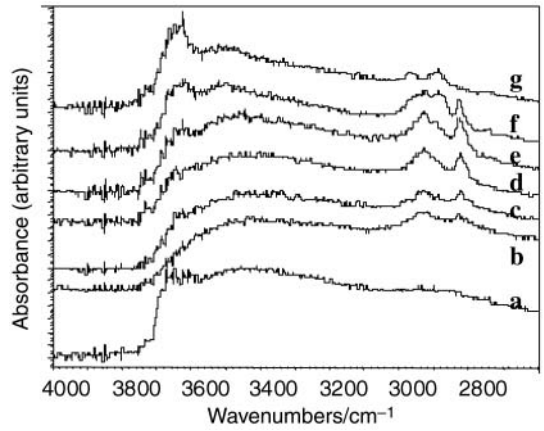

Fig. 11 FT-IR spectra arising from methanol adsorption on the $Fe_{1.8}Ga_{0.2}O_y$ sample in the 2600–4000 cm^{-1} region at different temperatures. a) Activation at 623 K, b) r.t., c) ev. 373 K, d) ev. 423 K, e) ev. 473 K, f) ev. 523 K and g) ev. 573 K (ev. = outgassing).

Study of the methanol adsorption. Methanol molecules were adsorbed on the surface of all Fe_xGa_{1-x} samples in order to deepen the knowledge of the reactivity of the Fe–Ga mixed oxides. FT-IR spectra obtained for the $Fe_{1.8}Ga_{0.2}$ sample at r.t. and after outgassing at different temperatures are compared in Figs. 10 and 11, as a representative example. At r.t. a doublet is found at 1033 and 1069 cm^{-1} together with a band situated at 1365 cm^{-1} (Fig. 10a), which can be associated with the δ_{OH} deformation and the ν_{OH} stretching bands of physisorbed methanol vapor in good agreement with the data reported by other authors.[30,31] Moreover, the ν_{OH} stretching band of surface OHs next to 3600 cm^{-1} appears without significant changes after methanol adsorption together with the ν_{CH} stretching bands at 2800 and 2900 cm^{-1} in the 2600–4000 cm^{-1} region (Fig. 11). A slight increase of temperature produces the sudden disappearance of the band at 1034 cm^{-1}, while that at 1067 cm^{-1} does so progressively. In parallel, a doublet appears at 1360 and 1370 cm^{-1} as well as a very sharp band at 1590 cm^{-1}. Both features are associated with formate species, ν_{as}(COO), δ(CH) and ν_s(COO), respectively.[32] On the other hand, the surface hydroxyl region disappears as a result of the interaction of methanol with the surface and a significant shift is observed, with a wide band appearing at 3400 cm^{-1}. This indicates the formation of H bonds and subsequent H^+ loss from the surface OH giving rise to methoxy species on the surface. After heating at 573 K, methanol converts fully to carbonate species and CO_2 (Fig. 10g) and the surface hydroxyl region appears well-defined again. The behavior observed for other samples shows that the methanol–surface interaction is stronger with increasing Ga content, with the δ_{OH} deformation band of methanol vapor appearing at higher wavenumbers. Nevertheless, the reactivity increases for low Ga contents, the highest activity being found for $Fe_{1.8}Ga_{0.2}$ where formate species are detected at 423 K.

These results indicate that Fe–Ga mixed oxides are suitable catalysts for the total oxidation of volatile organic compounds (VOCs). The increase in the activity of the Ga-doped samples (with respect to the Fe pure oxide) seems to be related to the increase in the Lewis acid strength, which implies that adsorbed methoxy species undergo a stronger interaction with the catalyst surface and are oxidized to CO_2 *via* formate–carbonate intermediates at lower temperatures. The presence of Brönsted acid sites probably has no effect on the catalytic pathway because methanol oxidation initiates with the H abstraction

from the hydroxyl group and formation of adsorbed methoxy species on Lewis acid sites.

Conclusions

The main conclusions found in this study are summarized below:

Fe–Ga mixed oxides synthesized by coprecipitation at controlled pH give rise to solid solutions in the entire range of Fe/Ga compositions, denoted as α-$(Fe,Ga)_2O_3$.

These solid solutions show good stability up to 800 °C and for Fe/Ga ratios < 3, due to the α–β phase transition of gallium oxide, which changes notably the structure.

Electronic spectra vary notably in intensity with increasing Ga content as a consequence of the progressive diffusion of Ga^{3+} into the α-Fe_2O_3 structure.

FT-IR spectra confirm the occurrence of Fe–Ga solid solutions with a significant broadening of all bands, which does not allow one to identify the bands of the Fe or Ga oxide spectra.

The surface of these materials is mainly made up of OH groups on octahedrally coordinated and bridging cations, with the latter being qualitatively more important, the FT-IR peaks of which shift towards higher wavenumbers with increasing Ga content.

Fe–Ga mixed oxides show weak Lewis acid sites whose strength increases upon increasing the Ga content. Also, Brönsted acid sites are present as indicated by the shifting of the band at 3600 cm^{-1} to 3300 cm^{-1} for the α-Ga_2O_3 sample, as a consequence of the formation of H bonds.

Methanol adsorption shows that samples with low Ga content exhibit higher reactivity, with the the methanol-to-formate conversion detected at 423 K, almost 80 K lower than for the other samples.

Acknowledgements

Part of this work has been supported by NATO (CRG-960316) and Junta de Castilla y León (ref[a]: SA37/98). J. M. G. A. and E. F. L. acknowledge MEC and Junta de Castilla y León, respectively, for FPI grants.

References

1 N. N. Greenwood and A. Earnshaw, *Chemistry of the Elements*, 5th edn., Butterworth Heinemann, Oxford, 1995, p. 278.
2 S. Geller, *J. Chem. Phys.*, 1960, **33**, 676.
3 V. Kanazirev, R. Dimitrova, G. L. Price, A. Yu. Kodakov, L. M. Kustov and V. B. Kazansky, *J. Mol. Catal.*, 1990, **70**, 111.
4 V. Kanazirev, G. L. Price and K. M. Dooley, *J. Chem. Soc., Chem. Commun.*, 1990, 712.
5 P. Mèriaudeau, G. Sapaly and C. Naccache, *J. Mol. Catal.*, 1993, **81**, 293.
6 K. Shimizu, A. Satsuma and T. Hattori, *Appl. Catal. B: Environ.*, 1998, **16**, 319.
7 A. Yu. Kodakov, L. M. Kustov, T. N. Bondarenko, A. A. Dergachev, V. B. Kazansky, Kh. M. Minachev, G. Borbely and H. K. Beyer, *Zeolites*, 1990, **10**, 603.
8 G. L. Price and V. Kanazirev, *J. Catal.*, 1990, **126**, 267.
9 A. P. Singh and K. R. Reddy, *Zeolites*, 1994, **14**, 291.
10 E. Lalik, X. Liu and J. Klinowski, *J. Phys. Chem.*, 1992, **96**, 805.
11 M. Baldi, V. Sanchez Escribano, J. M. Gallardo-Amores, F. Milella and G. Busca, *Appl. Catal. B: Environ.*, 1998, **17**, L-175.
12 V. Sanchez Escribano, J. M. Gallardo Amores, G. Busca, R. Ruano Casero and E. Pérez Bernal, *XXIII Reunion Iberica de Adsorsao, Evora, Portugal*, Abstracts book, pp. 35–38, 1998.
13 M. Lenglet, M. Bizi and C. K. Jorgensen, *J. Solid State Chem.*, 1990, **86**, 82.
14 G. Busca, G. Ramis, M. C. Prieto and V. Sanchez-Escribano, *J. Mater. Chem.*, 1993, **3**, 665.
15 M. C. Prieto, J. M. Gallardo-Amores, V. Sanchez-Escribano and G. Busca, *J. Mater. Chem.*, 1994, **4**, 1123.
16 V. Sanchez-Escribano, J. M. Gallardo-Amores, E. Finocchio, M. Daturi and G. Busca, *J. Mater. Chem.*, 1995, **5**, 1943.
17 J. M. Gallardo-Amores, V. S. Escribano and G. Busca, *J. Mater. Chem.*, 1999, **9**, 1161.
18 T. Moeller, *Química Inorgánica*, 2nd edn., Reverté S.A., Barcelona, 1988.
19 A. R. West, *Solid State Chemistry and its Applications*, 1st edn., John Wiley and Sons, New York, 1989.
20 C. J. Serna, J. L. Rendon and J. E. Iglesias, *Spectrochim. Acta*, 1982, **38A**, 797.
21 T. R. Burkholder, T. J. Yustein and L. J. Andrews, *J. Phys. Chem.*, 1992, **96**, 10189.
22 D. M. Sherman and R. G. Burns, *J. Geophys. Res.*, 1982, **87**, 169.
23 G. Busca, V. Lorenzelli, G. Ramis and R. J. Willey, *Langmuir*, 1993, **9**, 1492.
24 D. Dohy, G. Lucazeau and A. Revcolevschi, *J. Solid State Chem.*, 1982, **45**, 180.
25 B. Sulikowski, Z. Olejniczak and V. Cortes Corberan, *J. Phys. Chem.*, 1996, **100**, 10323.
26 V. Lorenzelli and G. Busca, *Mater. Chem. Phys.*, 1985, **131**, 261.
27 G. Busca, *Langmuir*, 1986, **2**, 577.
28 C. U. I. Odenbrand, J. G. M. Brandin and G. Busca, *J. Catal.*, 1992, **135**, 505.
29 G. Busca, *Catal. Today*, 1998, **41**, 191.
30 J. P. Gallas, PhD Thesis, University of Caen, 1984
31 G. Busca, P. F. Rossi, V. Lorenzelli, M. Benaissa, J. Travert and J. C. Lavalley, *J. Phys. Chem.*, 1985, **89**, 5433.
32 G. Busca, P. Forzatti, J. C. Lavalley and E. Tronconi, in *Catalysis by Acids and Bases*, ed. B. Imelik and J. C Vendrine, Elsevier Science, The Netherlands, 1985, p. 15.